

# Catalytic Oxidation of Alcohol via Nickel Phosphine Complexes with Pendant Amines

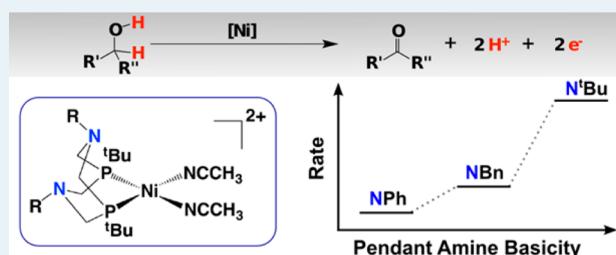
Charles J. Weiss, Parthapratim Das, Deanna L. Miller, Monte L. Helm, and Aaron M. Appel\*

Physical Sciences Division, Pacific Northwest National Laboratory, P.O. Box 999, MS K2-57, Richland, Washington 99352, United States

## Supporting Information

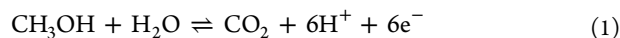
**ABSTRACT:** Nickel complexes were prepared with diphosphine ligands that contain pendant amines, and these complexes catalytically oxidize primary and secondary alcohols to their respective aldehydes and ketones. Kinetic and mechanistic studies of these prospective electrocatalysts were performed to understand what influences the catalytic activity. For the oxidation of diphenylmethanol, the catalytic rates were determined to be dependent on the concentration of both the catalyst and the alcohol and independent of the concentration of base and oxidant. The incorporation of pendant amines to the phosphine ligand results in substantial increases in the rate of alcohol oxidation with more electron-donating substituents on the pendant amine exhibiting the fastest rates.

**KEYWORDS:** alcohol oxidation, nickel, electrochemistry, catalysis, proton relay



## INTRODUCTION

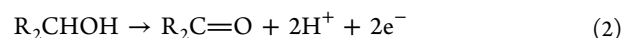
The intermittent availability of renewable electrical energy requires an efficient and economical means of energy storage to enable widespread utilization. One approach to the storage of renewable energy is the formation of carbon-based liquid fuels, such as alcohols, from the reduction of CO<sub>2</sub>. When energy is needed, the resulting carbon-based fuels, such as methanol and ethanol, can then be converted back to CO<sub>2</sub> (eq 1) electrochemically using fuel cells.<sup>1</sup> The production and utilization of alcohols for an energy storage cycle will require the development of effective electrocatalysts for these chemical transformations.



Molecular catalysts for the oxidation of alcohols are well-known;<sup>2</sup> however, molecular electrocatalysts for oxidation of alcohols for fuel storage cycles are much fewer in number.<sup>3</sup> To the best of our knowledge, all of the reported molecular electrocatalysts for alcohol oxidation require precious metals,<sup>3</sup> unlike reported catalysts for the chemical alcohol oxidation used in organic syntheses<sup>2e,i,4</sup> and Meerwein–Ponndorf–Verley (MPV) catalysts for transfer hydrogenation between alcohols and ketones or aldehydes.<sup>5</sup> For the electrocatalytic production and utilization of fuels, the movement of both electrons and protons is critical (eqs 1 and 2). The incorporation of proton relays in the second coordination sphere of transition metal complexes facilitates the movement of protons to and from the metal center, and this approach has been shown to be effective in the design of electrocatalysts for a variety of transformations.<sup>6</sup> First-row transition metal complexes containing cyclic diphosphine ligands with pendant amines have been

studied as electrocatalysts for the production<sup>7</sup> and oxidation<sup>7e,8</sup> of hydrogen and for the oxidation of formate.<sup>9</sup> The design and function of electrocatalysts for the oxidation of alcohols is expected to benefit from the incorporation of pendant amines due to the required movement of protons.

The focus of the present work is on the design and use of nickel diphosphine complexes as catalysts for the oxidation of alcohols, with an emphasis on the effects of incorporation of a pendant base. Our goal is to understand the factors that influence the first step (eq 2) of a multistep electrochemical oxidation of alcohols using these nickel catalysts, as this step will be critical to developing catalysts for the complete oxidation shown in eq 1. Due to the observed rates of alcohol oxidation being too slow to measure by typical diffusive electrochemical techniques, a chemical oxidant has been utilized as an electron acceptor in place of an electrode. Employing this proxy has enabled the use of *in operando* NMR spectroscopy to determine catalytic rates and reaction orders through directly observing reactant consumption and product formation. The results reported in this work provide the foundation and understanding needed for subsequent electrochemical studies using analogous catalysts.



Received: June 18, 2014

Revised: July 21, 2014

Published: July 23, 2014

## RESULTS

**Synthesis and Characterization.** Nickel(II) diphosphine complexes were prepared by the addition of  $P^R_2N^{R'}_2$  (1,5-*R'*-3,7-*R*-1,5-diaza-3,7-diphosphacyclooctane) or dcpe (dicyclohexylphosphinoethane) to  $Ni(CH_3CN)_6(BF_4)_2$ , which generated complexes of the formula  $Ni(P^{tBu}_2N^{R'}_2)(CH_3CN)_n(BF_4)_2$  ( $n = 2-3$ ;  $R = Ph$  (1),<sup>7h</sup>  $Bn$  (2),<sup>7h</sup>  $tBu$  (3)),  $Ni(dcpe)(CH_3CN)_2(BF_4)_2$  (4), and  $Ni(P^R_2N^{Bn}_2)_2(BF_4)_2$  ( $R = Cy$  (5)<sup>8f</sup> and  $Ph$  (6)<sup>10</sup>), as shown in Figure 1. A single ligand

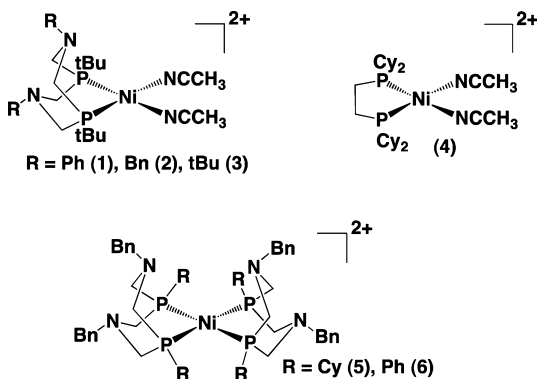


**Figure 1.** Nickel complexes used in the electrocatalytic oxidation of alcohols.

coordinated to the nickel in 1–4 due to the steric encumbrance of the phosphine substituents. The two new complexes 3 and 4 have been characterized by  $^1H$  and  $^{31}P$  NMR spectroscopy, X-ray crystallography (Figure 2), elemental analysis, and cyclic voltammetry (see the Supporting Information). Complex 3 has two coordinated solvent molecules, similar to 2 and distinct from 1, which was reported with three  $CH_3CN$  ligands.<sup>7h</sup> Complexes 3 and 4 exhibit reversible  $Ni(II/I)$  couples and irreversible  $Ni(I/0)$  couples similar to previously reported compounds 1 and 2.<sup>7h</sup>

**Catalytic Studies.** Complexes 1–6 were found to catalyze the oxidation of primary and secondary alcohols to aldehydes and ketones using triethylamine ( $Et_3N$ ) and decamethylferrocenium ( $Cp^*_2Fe^+$ ;  $Cp^* = Me_5C_5$ )<sup>11,12</sup> as the stoichiometric base and oxidant, respectively, in these model reactions (eq 3). The catalytic performances of complexes 1–6 were compared

using the oxidation of diphenylmethanol to benzophenone as a test reaction, with the results shown in Table 1.

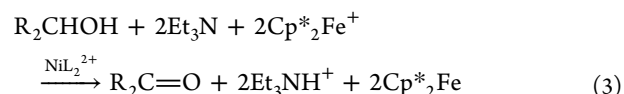


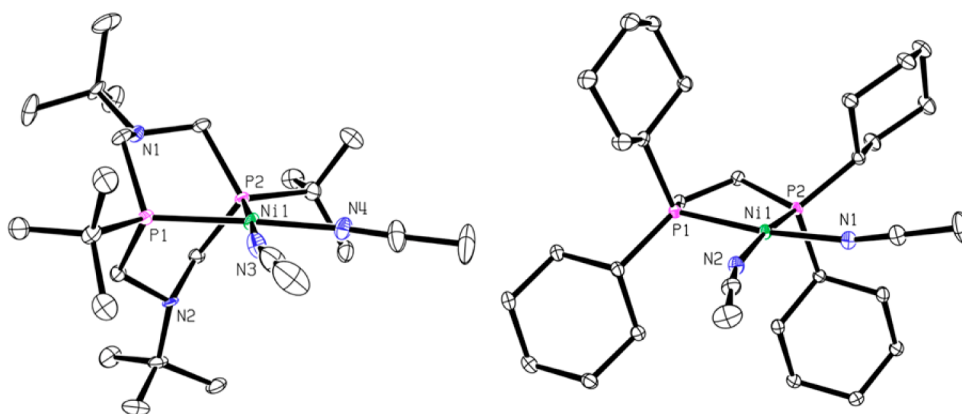
**Table 1.** Measured Turnover Frequencies for the Nickel-Catalyzed Oxidation of Diphenylmethanol to Benzophenone

entry	compound	TOF, $h^{-1a}$
1	$[Ni(P^{tBu}_2N^{Ph}_2)(CH_3CN)_3]^{2+}$ (1)	$9.4 \pm 3.2$
2	$[Ni(P^{tBu}_2N^{Bn}_2)(CH_3CN)_2]^{2+}$ (2)	$26.8 \pm 3.4$
3	$[Ni(P^{tBu}_2N^{tBu}_2)(CH_3CN)_2]^{2+}$ (3)	$114 \pm 5.2$
4	$[Ni(dcpe)(CH_3CN)_2]^{2+}$ (4)	$5.4 \pm 3.4$
5	$[Ni(P^{Cy}_2N^{Bn}_2)]^{2+}$ (5)	0.4
6	$[Ni(P^{Ph}_2N^{Bn}_2)]^{2+}$ (6)	<0.1

<sup>a</sup>Turnover frequencies are the initial rates of alcohol oxidation at  $25 \pm 0.5$  °C in  $CD_3CN$  with 0.10 equiv of catalyst, 1.9 equiv of  $Et_3N$ , and 1.9 equiv, thereby resulting in a maximum number of turnovers of 9.5.  $Cp^*_2FeBF_4$  versus diphenylmethanol. See the Supporting Information for full experimental details.

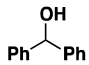
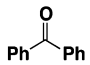
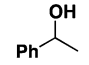
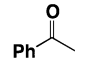
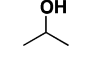
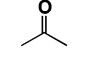
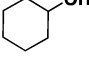
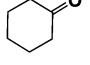
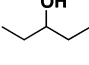
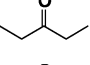
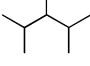
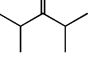
The complexes with two  $P^R_2N^{Bn}_2$  ligands, 5 and 6, were the slowest catalysts in this series, in spite of being active electrocatalysts for the oxidation of formate to  $CO_2$  (with turnover frequencies of  $9.6-12.5 s^{-1}$ ).<sup>9</sup> Rates for the oxidation of diphenylmethanol with these two complexes were found to improve significantly upon heating the reaction to 55 °C, at which temperature the rates increased to  $3.4 h^{-1}$  and  $60 h^{-1}$  for  $R = Ph$  and  $Cy$ , respectively.<sup>13</sup> The results with complexes 5 and 6 as well as the higher rates observed with complexes 1–4 are consistent with inhibition of catalysis in the presence of a second diphosphine ligand. In addition to the higher turnover frequencies observed for the monodiphosphine complexes, 1–4 ( $5.4-114 h^{-1}$ , Table 1), a 10-fold increase in rate is also observed with increasing the basicity of the pendant amine on the diphosphine ligand (Table 1, 1–3).<sup>14</sup> Furthermore, an appreciably lower rate is observed when no pendant amine is present, as indicated by the results with 4.

To study the effects of varying steric and electronic properties of the substrate, experiments were performed with additional alcohols, as shown in Table 2. Larger substituents on secondary, aliphatic alcohols resulted in decreased rates for the oxidation (Table 2, entries 3, 5, and 6), which is consistent with



**Figure 2.** Thermal ellipsoid plots rendered at 50% probability for the structures of the nickel complexes 3 (left) and 4 (right). Hydrogen atoms, anions, and noncoordinated solvent have been omitted for clarity.

**Table 2. Oxidation of Secondary Alcohols to Ketones Catalysed by  $[\text{Ni}(\text{P}^{\text{tBu}}_2\text{N}^{\text{Bn}}_2)(\text{CH}_3\text{CN})_2]^{2+}$  (**2**)<sup>a</sup>**

entry	alcohol	product	TOF, h <sup>-1b</sup>
1			26.8±3.4
2			24.4±2.4
3			29.4±5.2
5			40.9±10.6
6			12.4±2.6
7			8.0±2.4

<sup>a</sup>Turnover frequencies are the initial rates of alcohol oxidation at 25 ± 0.5 °C in CD<sub>3</sub>CN with 0.10 equiv of **2**, 1.9 equiv of Et<sub>3</sub>N, and 1.9 equiv of Cp\*<sub>2</sub>Fe<sup>+</sup>, thereby resulting in a maximum number of turnovers of 9.5. See the Supporting Information for full experimental details. <sup>b</sup>Uncertainty values are two standard deviations calculated from multiple kinetic runs.

a rate-limiting step that involves the binding of the alcohol to the metal.

To examine electronic effects while minimizing steric changes, the rate of oxidation of 4'-substituted α-methyl benzyl alcohols was measured with varying electronic donating and withdrawing substituents in the para position of the benzene ring (Table 3). For Br-, H-, and MeO-substituted alcohols

**Table 3. Ni(P<sup>tBu</sup><sub>2</sub>N<sup>Bn</sup><sub>2</sub>)(CH<sub>3</sub>CN)<sub>2</sub>(BF<sub>4</sub>)<sub>2</sub> (**2**)-Mediated Oxidation of Secondary Alcohols to Ketones<sup>a</sup>**

entry	substituent (X)	σ-value <sup>b15</sup>	TOF, h <sup>-1c</sup>
1	-Br	0.26	28.4 ± 14.8
2	-F	0.15	73.2 ± 20.4
3	-H	0.0	24.4 ± 2.4
4	-OMe	-0.12	25.9 ± 6.4
5	-NH <sub>2</sub>	-0.30	<sup>d</sup>

<sup>a</sup>Turnover frequencies are the initial rates of alcohol oxidation at 25 ± 0.5 °C in CD<sub>3</sub>CN with 0.10 mol equiv of nickel, 1.9 mol equiv of Et<sub>3</sub>N, and 1.9 mol equiv of Cp\*<sub>2</sub>FeBF<sub>4</sub> versus diphenylmethanol, thereby resulting in a maximum number of turnovers of 9.5. <sup>b</sup>σ-Values quantify the electronic effects of the para substituent with positive values having a net electron withdrawing effect and negative values having a net electron donating effect. <sup>c</sup>Uncertainty values are two standard deviations calculated from multiple kinetic runs. <sup>d</sup>Little or no alcohol oxidation observed.

(Table 3, entries 1, 3, and 4), an average TOF of ~26 h<sup>-1</sup> was observed with minimal variation, suggesting no significant electronic effect. Based on the lack of significant variation in the rates using the Br-, H-, and MeO-substituted alcohols, the deviation of catalytic rates for F- and NH<sub>2</sub>-substituted alcohols is not expected to result from differences in simple electronics. In the case of the amine-substituted alcohol, the reaction may be impeded by possible binding of the amine functionality to the metal center.

The analogous oxidation reactions were also performed with the primary alcohols methanol, ethanol, and benzyl alcohol (eq 4) using **2** as the catalyst. For methanol, the expected product, formaldehyde was not observed; however, methylformate was observed in substoichiometric quantities.<sup>16,17</sup> For ethanol, acetaldehyde was formed, based on the observation of a singlet at 9.69 ppm in the <sup>1</sup>H NMR spectrum. However, this product was quickly converted to ethyl acetate, presumably from either further oxidation to acetate and subsequent esterification with ethanol or reaction of two equivalents of acetaldehyde to generate this four electron oxidized product. In contrast to the results with ethanol, oxidation of benzyl alcohol (81.4 ± 10.0 h<sup>-1</sup>) was observed to produce benzaldehyde, with little or no benzyl benzoate observed. When a similar study is performed using a 1:1 mixture of benzaldehyde and ethanol, a 2:7 mixture of ethyl acetate and ethyl benzoate forms.



**Mechanistic Investigations.** To understand what factors limit the catalytic rates, the oxidation of diphenylmethanol catalyzed by **2** was studied as a function of the reagent concentrations, using Et<sub>3</sub>N and Cp\*<sub>2</sub>FeBF<sub>4</sub> as the base and oxidant, respectively. Increasing the concentration of **2** over the range of 0.9–7.4 mM resulted in a linear increase in the rate of oxidation of the alcohol (Figure 3, left), consistent with first-order dependence on the concentration of the catalyst. The turnover frequency increased linearly with increasing concentration of diphenylmethanol over the range of 10–218 mM (Figure 3, right), indicating a first-order dependence on the concentration of alcohol. In the presence of excess diphenylmethanol, benzophenone was produced at a constant rate until all base and oxidant were consumed (Figure 4). This lack of dependence on the diminishing concentrations of Et<sub>3</sub>N and Cp\*<sub>2</sub>FeBF<sub>4</sub> indicates that the reaction rate is independent of the concentrations of these two reagents. No significant change in initial rate was observed when the oxidation of diphenylmethanol catalyzed by **2** was examined with ~4× higher concentration of Et<sub>3</sub>N (7.6 mol equiv, 340 mM), further supporting that the catalytic reaction is independent of base concentration. Combined with the first-order dependence on the concentrations of diphenylmethanol and the catalyst, these results are consistent with the rate law in eq 5.

$$\text{Rate}_{\text{initial}} = k_{\text{obs}}[\mathbf{2}][\text{diphenylmethanol}] \quad (5)$$

The observed rate law is consistent with the binding of the alcohol limiting the rate due to either slow binding or unfavorable binding that precedes a rate-determining transition state. The first-order dependence of the rate on alcohol concentration was observed over the entire course of the reaction, in the presence of excess diphenylmethanol (5 times as much diphenylmethanol relative to the base and oxidant). However, when equally limiting concentrations of alcohol, base, and oxidant are used, the apparent rate law changed after ~50% conversion (Figure S9). No significant change in rate was observed in the presence of added benzophenone, suggesting that the change in rate is not due to product inhibition. Due to the constant rate of diphenylmethanol oxidation with excess alcohol, catalyst deactivation is also unlikely. The observed slowing of the reaction may be due to a more complex rate law than shown in eq 5, perhaps resulting from competition between multiple catalytic pathways. One possible source of additional catalytic pathways is the variable number of solvent

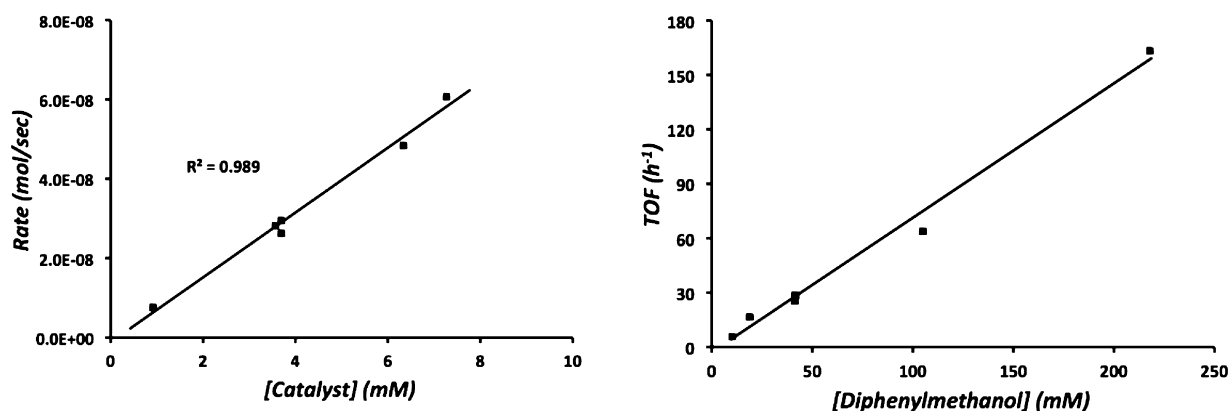


**Figure 3.** Plot of catalytic rate versus [catalyst] (mM) (left) and versus [diphenylmethanol] (mM) (right) for the  $\text{Ni}(\text{P}^{\text{tBu}}_2\text{N}^{\text{Bn}})_2(\text{CH}_3\text{CN})_2(\text{BF}_4)_2$  (**2**)-catalyzed oxidation of diphenylmethanol to benzophenone at 25 °C with  $\text{Et}_3\text{N}$  and  $\text{Cp}^*\text{FeBF}_4$ .

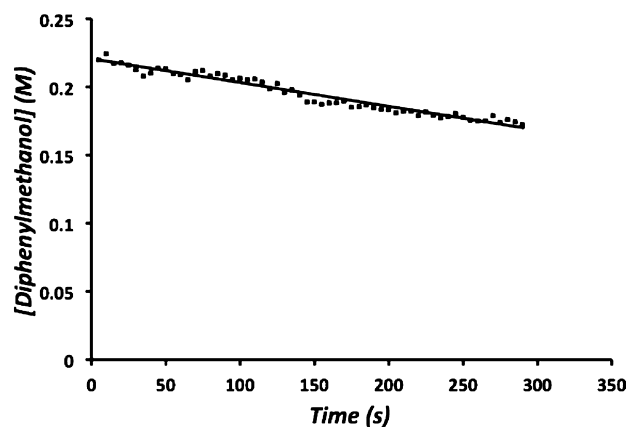


**Figure 4.** Plot of time (s) versus [diphenylmethanol] (M) for the  $\text{Ni}(\text{P}^{\text{tBu}}_2\text{N}^{\text{Bn}})_2(\text{CH}_3\text{CN})_2(\text{BF}_4)_2$  (**2**)-catalyzed (4 mM) oxidation of diphenylmethanol to benzophenone at 25 °C with  $\text{Et}_3\text{N}$ ,  $\text{Cp}^*\text{FeBF}_4$ , and a 5-fold excess of diphenylmethanol versus base and oxidant. The reaction is complete after 300 s due to complete consumption of base and oxidant. The linear trend indicates that the excess alcohol has resulted in a pseudo-zero-order reaction.

molecules coordinated to the metal center<sup>7h,18</sup> and therefore possible variation in the number of alcohols or bases that bind to the nickel at some point in the catalytic cycle.

In contrast with the first-order dependence on alcohol concentration for diphenylmethanol, the analogous oxidation of 2-propanol under the same conditions was observed to have a half-order dependence on the concentration of alcohol over the entire course of the reaction (see Figure S11). The dependence of the catalytic rate on the concentration of alcohol varied over the range of 0.5 to 1 for the studied alcohols.

When  $i\text{Pr}_2\text{EtN}$  was used as the base for the oxidation of diphenylmethanol, the catalytic rate with **2** increased to  $78.4 \pm 7.2 \text{ h}^{-1}$ . This rate is approximately three times faster than the rate with  $\text{Et}_3\text{N}$ , despite the observed independence from the concentration of  $\text{Et}_3\text{N}$ . The  $^1\text{H}$  NMR spectra of **2** in the presence of 3.7 equiv of  $\text{Et}_3\text{N}$  (Figure 5) contains resonances for the base that are shifted downfield by 0.07–0.18 ppm, suggesting base binding to the nickel center. The same experiment with  $i\text{Pr}_2\text{EtN}$  results in no shifting of the base resonances. The  $^{31}\text{P}$  NMR spectra of **2** in the presence of  $\text{Et}_3\text{N}$  for the above experiments contain two new species in addition

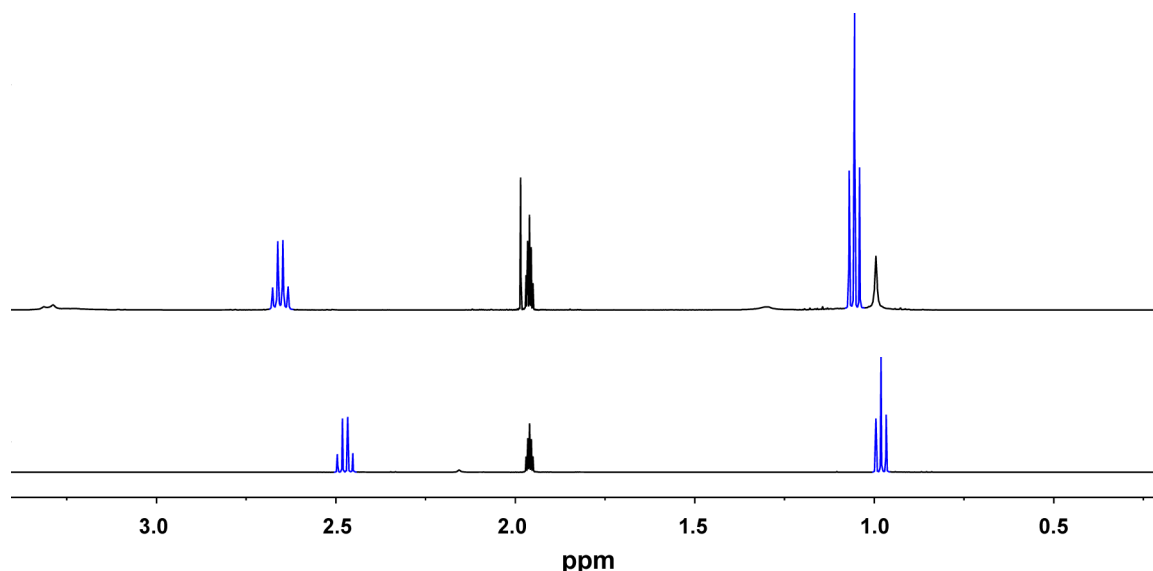


**Figure 5.**  $^1\text{H}$  NMR (500 MHz) spectra in  $\text{CD}_3\text{CN}$  (1.94 ppm) of  $\text{Et}_3\text{N}$  (blue) without a nickel complex (bottom) and  $\text{Et}_3\text{N}$  (2.0  $\mu\text{L}$ ,  $1.4 \times 10^{-5}$  mol) with  $\text{Ni}(\text{P}^{\text{tBu}}_2\text{N}^{\text{Bn}})_2(\text{CH}_3\text{CN})_2(\text{BF}_4)_2$  (**2**) (2.9 mg,  $3.8 \times 10^{-6}$  mol) (top). The downfield shift of the  $\text{Et}_3\text{N}$  resonances suggests an interaction between the amine and the nickel complex.

to the starting complex, whereas the analogous  $^{31}\text{P}$  NMR spectra in the presence of  $^i\text{Pr}_2\text{EtN}$  contain only the starting complex. These results are consistent with hindered binding of  $^i\text{Pr}_2\text{EtN}$  due to increased sterics. To test if  $\text{Et}_3\text{N}$  displaces one of the  $\text{CH}_3\text{CN}$  ligands in complexes 1–3,  $\text{Et}_3\text{N}$  and **1** were dissolved in  $\text{CD}_2\text{Cl}_2$ , leading to the liberation of acetonitrile concurrent with the binding of  $\text{Et}_3\text{N}$  (Figure S19). For comparison to the alkylamine bases,  $\text{KOH}$  and  $^t\text{Bu-P4}$  phosphazene were also tested and found to be effective for the oxidation of diphenylmethanol; however, problems with solubility prevented quantification of catalytic rates using these bases.

**Low Temperature Stoichiometric Studies.** The addition of excess benzyl alcohol and  $\text{Et}_3\text{N}$  to **1** and **2** at  $-40\text{ }^\circ\text{C}$  resulted in the formation of nickel hydrides, with resonances consistent with previous  $\text{Ni(II)}$ -hydride complexes with two  $\text{P}_2\text{N}_2$  ligands.<sup>19</sup> For **2**, the resulting hydride was not observed to be stable when warmed to  $25\text{ }^\circ\text{C}$ ; however, for the hydride from the reaction of **1** was stable at  $25\text{ }^\circ\text{C}$  for over an hour. The analogous reaction with **3** did not result in observable hydride resonances. An X-ray crystal structure of a tetrahedral complex of nickel with two  $\text{P}^t\text{Bu}_2\text{N}^{\text{Ph}}_2$  ligands was obtained (Figure 6),

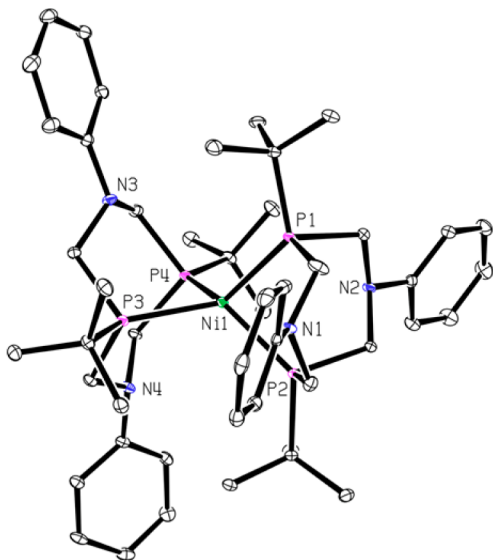


**Figure 6.** Thermal ellipsoid plots of  $\text{Ni}(\text{P}^t\text{Bu}_2\text{N}^{\text{Ph}}_2)_2(\text{BF}_4)$  rendered at 50% probability. Hydrogen atoms, anions, and noncoordinated solvent have been omitted for clarity.

but there was no indication of the presence of a hydride in the crystal structure. Similarly, no hydride resonance was observed in the  $^1\text{H}$  NMR spectrum collected by dissolving additional crystals from the same batch used to obtain the X-ray structure, suggesting the identity of the complex was the  $\text{Ni(I)}$  complex,  $\text{Ni}(\text{P}^t\text{Bu}_2\text{N}^{\text{Ph}}_2)_2(\text{BF}_4)$ , rather than the analogous  $\text{Ni(II)}$ -hydride.

## DISCUSSION

The proposed catalytic cycle for the oxidation of alcohols by complexes 1–3 is shown in Scheme 1. Starting from the upper left, the first step is proposed as the coordination of the alcohol to the metal complex, followed by deprotonation to form the metal-bound alkoxide. Given that trialkylamines are not typically strong enough bases to deprotonate alcohols,<sup>20</sup> the deprotonation step is proposed to be enabled by the increase in

acidity resulting from coordination of the alcohol to the metal center.

The initial binding of the alcohol appears to be an unfavorable equilibrium that precedes deprotonation. No alcohol binding is observed by  $^{31}\text{P}$  NMR spectroscopy when **2** and diphenylmethanol are mixed in the absence of base (see the Supporting Information). The observed reaction order with respect to alcohol was found to be first-order for diphenylmethanol, whereas it was approximately half-order for 2-propanol. The variation in apparent reaction order with respect to alcohol concentration may be the result of multiple competing reaction pathways with different orders with respect to alcohol concentration.

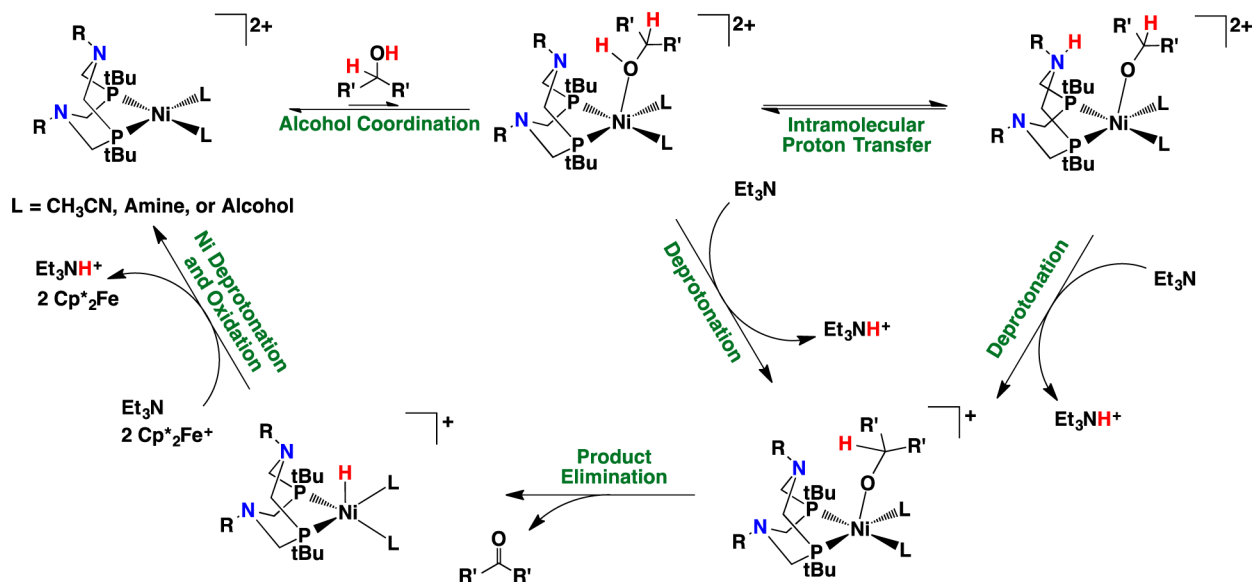
The lack of variation in catalytic rates with different electron withdrawing and donating substituents on the substrates (Table 3) suggests, if the mechanism proposed in Scheme 1 is correct, that there is a balance between the alcohol binding strength and the acidity of the resulting metal-bound alcohol. The more donating substituents may result in improved binding of the alcohol to the metal center but would also be expected to yield a less acidic coordinated alcohol. Based on the lack of variation for the methoxy- and bromo-substituted alcohols relative to the unsubstituted equivalent (see Table 3), these two effects appear to be equally opposed.

While the rate of oxidation of diphenylmethanol by **2** is independent of base concentration, the analogous reaction using the complex without a pendant amine, **4**, is approximately first-order with respect to the concentration of  $\text{Et}_3\text{N}$  (see the Supporting Information). These two results suggest that deprotonation influences the rate-determining step, but that the complex without a pendant amine is dependent upon exogenous base for this step. The presence of the pendant base appears to be responsible for the observed base concentration independence for **2**.

The subsequent steps are proposed to involve the net transfer of a hydride from the bound alkoxide to the metal complex, followed by oxidation and deprotonation to return to the starting  $\text{Ni(II)}$  species. The catalytic studies provide very little information about these steps, given that they are after the rate-determining step. However, the formation of nickel-hydride species is supported by the observation of hydrides in stoichiometric reactions with alcohol and base at low temperature. This observation is consistent with the mechanism proposed in Scheme 1.

The pendant base within the ligand appears to play an important role in the catalytic reaction, as the rates are higher with the pendant amine and increase with increasing basicity of the ligand. The pendant amine may be involved in the transfer of the hydrogen from carbon to nickel through a proton-coupled electron transfer reaction,<sup>9b</sup> or the pendant amine may be involved in the oxidation and deprotonation steps that convert the proposed hydride back to the  $\text{Ni(II)}$  complex.<sup>21</sup> Regardless of the precise mechanism, the catalytic rate of the pendant amine containing complexes is independent of the concentration of either oxidant or base, and so these proton and electron transfer steps that are later in the cycle do not appear to be limiting.

**Summary and Conclusions.** Homogeneous nickel phosphine complexes were prepared and found to catalyze the oxidation of primary and secondary alcohols to their respective aldehydes and ketones. The results of mechanistic studies are consistent with rate-limiting binding of the alcohol to the metal center, followed by deprotonation of the metal-bound alcohol.

Scheme 1. Proposed Catalytic Cycle for the Oxidation of Alcohols Using  $[\text{Ni}(\text{P}^{\text{tBu}}_2\text{N}^{\text{R}}_2)(\text{CH}_3\text{CN})_2]^{2+}$  (2)

The addition of pendant amines to the phosphine ligand results in substantial increases in the rate of alcohol oxidation. While the precise nature of the rate enhancement by the pendant amine is not yet clear, variation of substituents at the pendant amine has a significant effect on upon catalytic rates. These studies demonstrate that alcohol oxidation is possible using these complexes, which is an essential first step in developing electrocatalysts based on this platform. Additional studies are underway, including the examination of this reaction by electrochemical methods.

## EXPERIMENTAL SECTION

**General Procedures.** Syntheses were performed under dry N<sub>2</sub> using a glovebox and standard Schlenk techniques. Protio solvents were purchased as anhydrous from Alfa-Aesar, VWR, and Fisher further dried using activated alumina columns and stored under N<sub>2</sub>. Acetonitrile-*d*<sub>3</sub> and methylene chloride-*d*<sub>2</sub> (Cambridge Isotope Laboratories, 99+ atom % D) were dried over CaH<sub>2</sub> and degassed under high-vacuum (10<sup>-6</sup> Torr) before being distilled and stored under dry N<sub>2</sub> until use. Paraformaldehyde, 1,2-bis(dicyclohexylphosphino)ethane (dcpe), <sup>t</sup>Bu-P<sub>4</sub> phosphazene, bis(pentamethylcyclopentadienyl)ferrocene, *p*-benzoquinone, and 1,3-dichloropropane were purchased from Aldrich and Alfa Aesar and used as received. All other phosphines were purchased from Strem. Triethylamine, ethyldiisopropylamine, 1,3,5-trimethoxybenzene, alcohols, ketones, and benzaldehyde were purchased from Aldrich, degassed under vacuum, and dried over multiple beds of activated 3 Å molecular sieves (liquids) or by pulling under vacuum (10<sup>-3</sup> Torr) overnight (solids). Compounds Ni(CH<sub>3</sub>CN)<sub>6</sub>(BF<sub>4</sub>)<sub>2</sub>,<sup>22</sup> P<sup>tBu</sup><sub>2</sub>N<sup>Bn</sup><sub>2</sub>,<sup>7h</sup> P<sup>tBu</sup><sub>2</sub>N<sup>Ph</sup><sub>2</sub>,<sup>7h</sup> P<sup>tBu</sup><sub>2</sub>N<sup>tBu</sup><sub>2</sub>,<sup>23</sup> Ni(P<sup>tBu</sup><sub>2</sub>N<sup>Bn</sup><sub>2</sub>)(CH<sub>3</sub>CN)<sub>2</sub>(BF<sub>4</sub>)<sub>2</sub> (2), and Ni(P<sup>tBu</sup><sub>2</sub>N<sup>Ph</sup><sub>2</sub>)(CH<sub>3</sub>CN)<sub>3</sub>(BF<sub>4</sub>)<sub>2</sub> (1) were synthesized by literature-reported procedures.<sup>7h</sup> The identity of ketones, benzaldehyde, and esters produced in catalytic oxidation reactions were confirmed by comparing the <sup>1</sup>H and <sup>13</sup>C NMR spectra against those of commercially obtained samples or literature values.<sup>24</sup> The <sup>1</sup>H, <sup>13</sup>C, and <sup>31</sup>P NMR spectra were collected on a Varian Inova 500 MHz spectrometer at 25 °C unless otherwise indicated. The temperature for kinetic experiments was determined by an

external methanol temperature calibration standard. The <sup>1</sup>H and <sup>13</sup>C NMR spectra are referenced versus tetramethylsilane (0.00 ppm) using internal CD<sub>3</sub>CN (<sup>1</sup>H: 1.94 ppm; <sup>13</sup>C: 118.69/1.39 ppm) and CD<sub>2</sub>Cl<sub>2</sub> (<sup>1</sup>H: 5.32 ppm; <sup>13</sup>C: 54.00) solvent resonances, while <sup>31</sup>P NMR spectra are referenced against a H<sub>3</sub>PO<sub>4</sub> external standard (0.0 ppm).

**Electrochemical Procedure.** Cyclic voltammetry was performed with 4–5 mM nickel complex dissolved in 1.0 mL solution of 0.1 M nBu<sub>4</sub>NPF<sub>6</sub> in CH<sub>3</sub>CN as the supporting electrolyte. All potentials were measured with a CH Instruments model 620D or 660C potentiostat and reported versus Cp<sub>2</sub>Fe<sup>+0</sup> (0.0 V). Measurements were performed using standard three-electrode cell containing a 1 mm PEEK-encased glassy carbon working electrode (Cypress Systems EE040), a 3 mm glassy carbon rod (Alfa) as the counter electrode, and a silver wire suspended in electrolyte solution and separated from the analyte solution by a Vycor frit as the pseudoreference electrode. Prior to the acquisition of each voltammogram, the working electrode was polished using 0.1 μm γ-alumina (BAS CF-1050) and rinsed with CH<sub>3</sub>CN.

**Synthesis of Ni(P<sup>tBu</sup><sub>2</sub>N<sup>tBu</sup><sub>2</sub>)(CH<sub>3</sub>CN)<sub>2</sub>(BF<sub>4</sub>)<sub>2</sub> (3).** Ni(CH<sub>3</sub>CN)<sub>6</sub>(BF<sub>4</sub>)<sub>2</sub> (110 mg, 0.230 mmol) and P<sup>tBu</sup><sub>2</sub>N<sup>tBu</sup><sub>2</sub> (183 mg, 0.489 mmol) were dissolved in 5 mL of acetonitrile and stirred for 2 h resulting in a deep red solution. The solution was filtered and concentrated to approximately 1 mL. The product was crystallized by ether diffusion at 21 °C to yield deep red crystalline material (24.4 mg, 0.0334 mmol, 14.5% yield). <sup>1</sup>H NMR (CD<sub>3</sub>CN, 25 °C): δ 4.07–3.64 (bs, 4H, CH<sub>2</sub>), 3.51–3.37 (m, 4H, CH<sub>2</sub>), 1.96 (s, 6H, CH<sub>3</sub>CN) 1.37 (s, 18H, C(CH<sub>3</sub>)<sub>3</sub>), 1.20 (s, 18H, C(CH<sub>3</sub>)<sub>3</sub>). <sup>1</sup>H NMR (CD<sub>3</sub>CN, –40 °C): δ 3.92–3.70 (bs, 4H, NCH<sub>2</sub>P), 3.56–3.44 (m, 4H, NCH<sub>2</sub>P), 1.96 (s, acetonitrile) 1.42 (s, 18H, C(CH<sub>3</sub>)<sub>3</sub>), 1.25 (s, 18H, C(CH<sub>3</sub>)<sub>3</sub>). <sup>31</sup>P{<sup>1</sup>H} NMR (CD<sub>3</sub>CN, –40 °C): δ 26.7 (bs). Anal. Calcd For C<sub>26</sub>H<sub>53</sub>B<sub>2</sub>F<sub>8</sub>N<sub>5</sub>NiP<sub>2</sub>: C, 42.78; H, 7.32; N, 9.59. Found: C, 42.77; H, 7.28; N, 10.58. CV (0.1 M nBu<sub>4</sub>NPF<sub>6</sub> in CH<sub>3</sub>CN, scan rate 100 mV/s): E<sub>1/2</sub>, V vs Fc<sup>+0</sup> (ΔE<sub>p</sub>, mV) –0.75 (103), –1.79 (irrev).

**Synthesis of Ni(dcpe)(CH<sub>3</sub>CN)<sub>2</sub>(BF<sub>4</sub>)<sub>2</sub> (4).** Ni(CH<sub>3</sub>CN)<sub>6</sub>(BF<sub>4</sub>)<sub>2</sub> (133 mg, 0.278 mmol) and dcpe (128 mg, 0.303 mmol) were dissolved in 5 mL of acetonitrile and stirred

for 90 min resulting in a yellow solution. The solution was concentrated to approximately 2 mL, and ether was diffused overnight at 21 °C to yield yellow crystals (152 mg, 0.197 mmol, 70.9% yield).  $^1\text{H}$  NMR ( $\text{CD}_3\text{CN}$ , 25 °C):  $\delta$  2.31–2.23 (m, 4H, Cy), 2.22–2.12 (m, 4H, Cy), 2.12–2.06 (m, 4H,  $\text{CH}_2\text{P}$ ), 2.01–1.89 (m, 8H, Cy), 1.98–1.95 (m,  $\text{CH}_3\text{CN}$ ), 1.89–1.81 (m, 4H, Cy), 1.79–1.72 (m, 4H, Cy), 1.63–1.27 (m, 20H, Cy).  $^{31}\text{P}\{^1\text{H}\}$  NMR ( $\text{CD}_3\text{CN}$ , 121 MHz 25 °C):  $\delta$  98.8 (s). Anal. Calcd For  $\text{C}_{30}\text{H}_{54}\text{B}_2\text{F}_8\text{N}_2\text{NiP}_2(\text{CH}_3\text{CN})$ : C, 49.40; H, 7.38; N, 5.40. Found: C, 49.05; H, 7.40; N, 5.16. CV (0.1 M  $\text{nBu}_4\text{NPF}_6$  in  $\text{CH}_3\text{CN}$ , scan rate 100 mV/s):  $E_{1/2}$ , V vs  $\text{Fc}^{+/0}$  ( $\Delta E_p$ , mV)  $-0.95$  (76),  $-1.65$  (irrev).

**Synthesis of  $\text{Cp}^*_2\text{FeBF}_4$ .** Using a similar procedure as described in the literature,<sup>25</sup> bis(pentamethylcyclopentadienyl)ferrocene (0.979 g, 3.00 mmol) and p-benzoquinone (0.649 g, 6.00 mmol) were loaded into a 250 mL Erlenmeyer flask in open air and dissolved in 100 mL of diethyl ether. To the solution was added dropwise 1.7 mL of  $\text{HBF}_4(\text{Et}_2\text{O})$  to immediately form a green precipitate, and the solution was stirred for an additional 10 min before filtering and washing with diethyl ether (400 mL). The solid was dried under vacuum to yield a green powder (1.18 g, 2.86 mmol, 95% yield). Anal. Calcd For  $\text{C}_{20}\text{H}_{30}\text{BF}_4\text{Fe}$ : C, 58.15; H, 7.32. Found: C, 58.32; H, 7.11.

**Synthesis of  $^t\text{Bu}_2\text{P}(\text{CH}_2)_3\text{P}^t\text{Bu}_2$ .** In a 50 mL Schlenk flask, a solution of  $^t\text{Bu}_2\text{PH}$  (1.6 g, 11 mmol) in 10 mL hexanes was treated dropwise with  $\text{nBuLi}$  solution in hexanes (2.5 M, 4.4 mL, 11 mmol) and stirred for 1 h to form a white, insoluble powder. The solvent was removed under vacuum, and the white product was dissolved in 10 mL of THF. The yellow solution was cooled to  $-78$  °C, and 1,3-dichloropropane (0.61 g, 5.4 mmol) was added dropwise. After 15 min, the solution was allowed to warm to room temperature and stir for an additional 17 h. The solvent was removed under vacuum, and the product was extracted with 30 mL hexanes and filtered. Removal of solvent yielded a pale yellow, viscous oil (1.41 g, 4.24 mmol, 79% yield).  $^1\text{H}$  NMR ( $\text{C}_6\text{D}_6$ , 23 °C, 300 MHz):  $\delta$  2.13–1.95 (m, 2H,  $\text{CH}_2\text{CH}_2\text{CH}_2$ ), 1.68–1.58 (m, 4H,  $\text{PCH}_2$ ), 1.25–1.17 (m, 36H,  $(\text{CH}_3)_3\text{CP}$ ).  $^{31}\text{P}\{^1\text{H}\}$  NMR ( $\text{C}_6\text{D}_6$ , 23 °C, 121 MHz):  $\delta$  26.3 (s).

**Typical Kinetic Procedure.** A 1.0 mL  $\text{CD}_3\text{CN}$  solution of catalyst ( $4.2 \times 10^{-6}$  mol), alcohol ( $4.2 \times 10^{-5}$  mol),  $\text{Cp}^*_2\text{FeBF}_4$  (32 mg,  $7.7 \times 10^{-5}$  mol), and 1,3,5-trimethoxybenzene internal standard (10–20 mg) was loaded into an NMR tube and sealed with a rubber septum. Triethylamine (11  $\mu\text{L}$ ,  $7.8 \times 10^{-5}$  mol) was injected into the NMR tube, and the contents were mixed by inversion before the tube was promptly inserting into a  $25.0 \pm 0.5$  °C NMR spectrometer. Single-scan  $^1\text{H}$  NMR spectra were collected at regular intervals with no spinning to minimize crystallization of generated  $\text{Cp}^*_2\text{Fe}$  on the NMR tube wall. Kinetic measurements were obtained by integrating product or alcohol  $^1\text{H}$  NMR resonances relative to the 1,3,5-trimethoxybenzene internal integration standard. Initial rates were measured by linear fit of alcohol consumption at the start of the reaction. Turnover-frequencies were calculated using the following eq 6 and reported as the average of multiple experiments. Uncertainties are two standard deviations calculated from three or more experiments.

$$\text{TOF (h}^{-1}\text{)} = \frac{\text{Alcohol Oxidation (mol/s)}}{\text{Catalyst (mol)}} \times 3600 \text{ s/h} \quad (6)$$

No alcohol oxidation is observed in the absence of nickel catalysts. The  $\text{Ni}(\text{CH}_3\text{CN})_6(\text{BF}_4)_2$  complex does not catalyze 2-propanol oxidation, indicating that the phosphine ligand is required for the reaction. No  $\text{H}_2$  gas has been observed in the  $^1\text{H}$  NMR spectra of alcohol oxidation reactions in the present study. Noncatalytic oxidation of 2-propanol to acetone is observed without chemical oxidant in the presence of **2** and  $\text{Et}_3\text{N}$ . The product of this reaction appears to be paramagnetic based on the NMR spectra, and the stoichiometry is consistent with Ni(I), in that only one-half equivalent of alcohol is oxidized.

**Hydride Formation.** A 1.0 mL acetonitrile solution of complexes **1–3** ( $1.6 \times 10^{-5}$  mol) and benzyl alcohol (6.0  $\mu\text{L}$ ,  $5.8 \times 10^{-5}$  mol) was loaded into an NMR tube sealed with a rubber septum and placed in a  $-40$  °C NMR spectrometer. The cold sample was briefly removed from the spectrometer to inject  $\text{Et}_3\text{N}$  (15.0  $\mu\text{L}$ ,  $1.08 \times 10^{-4}$  mol), mix by inversion, and promptly return to the spectrometer at  $-40$  °C. The reactions were monitored NMR spectroscopy over the course of multiple hours.

**X-ray Structural Analyses.** A single crystal of  $\text{Ni}(\text{P}^t\text{Bu}_2\text{N}^t\text{Bu}_2)(\text{CH}_3\text{CN})_2(\text{BF}_4)_2$  (**3**),  $\text{Ni}(\text{dcpe})(\text{CH}_3\text{CN})_2(\text{BF}_4)_2$  (**4**), or  $\text{Ni}(\text{P}^t\text{Bu}_2\text{N}^{\text{Ph}}_2)(\text{BF}_4)_2$  was placed on a nylon loop with Paratone-N oil and then mounted on a Bruker APEX-II CCD diffractometer for data collection at 140 K for **3** and 100 K for **4**. Using Olex2,<sup>26</sup> the structure for **3** and  $\text{Ni}(\text{P}^t\text{Bu}_2\text{N}^{\text{Ph}}_2)(\text{BF}_4)_2$  was solved with the olex2.solve<sup>27</sup> structure solution program using Charge Flipping. The structure of **4** was solved using direct methods within the ShelXS program package. Both crystals were refined with the ShelXL<sup>28</sup> refinement package using Least Squares minimization. All hydrogen atoms were placed at idealized positions.

## ■ ASSOCIATED CONTENT

### 📄 Supporting Information

Experimental procedures, control experiments, kinetic data, NMR spectra, and crystallographic data. This material is available free of charge via the Internet at <http://pubs.acs.org>.

## ■ AUTHOR INFORMATION

### ✉ Corresponding Author

\*E-mail: [aaron.appel@pnnl.gov](mailto:aaron.appel@pnnl.gov).

### Notes

The authors declare no competing financial interest.

## ■ ACKNOWLEDGMENTS

We thank Dr. John C. Linehan, Prof. Elliott B. Hulley, Dr. Jonathan M. Darmon, and Dr. Elizabeth L. Tyson for helpful discussions. Research by C.J.W., P.D., D.L.M., and A.M.A. was supported by the US Department of Energy, Office of Basic Energy Sciences, Division of Chemical Sciences, Geosciences & Biosciences. Research by M.L.H. was supported as part of the Center for Molecular Electrocatalysis, an Energy Frontier Research Center funded by the U.S. Department of Energy, Office of Science, Basic Energy Sciences. Pacific Northwest National Laboratory is operated by Battelle for the US Department of Energy.

## ■ REFERENCES

- (1) Sundmacher, K. *Ind. Eng. Chem. Res.* **2010**, *49*, 10159–10182.
- (2) (a) Sheeba, M. M.; Muthu Tamizh, M.; Farrugia, L. J.; Endo, A.; Karvembu, R. *Organometallics* **2014**, *33*, 540–550. (b) Zhang, G.;

- Vasudevan, K. V.; Scott, B. L.; Hanson, S. K. *J. Am. Chem. Soc.* **2013**, *135*, 8668–8681. (c) Balaraman, E.; Khaskin, E.; Leitius, G.; Milstein, D. *Nat. Chem.* **2013**, *5*, 122–125. (d) Yang, X. *ACS Catal.* **2013**, *3*, 2684–2688. (e) Hoover, J. M.; Ryland, B. L.; Stahl, S. S. *J. Am. Chem. Soc.* **2013**, *135*, 2357–2367. (f) Schley, N. D.; Dobreiner, G. E.; Crabtree, R. H. *Organometallics* **2011**, *30*, 4174–4179. (g) Brink, G.-J. t.; Arends, I. W. C. E.; Sheldon, R. A. *Science* **2000**, *287*, 1636–1639. (h) Peterson, K. P.; Larock, R. C. *J. Org. Chem.* **1998**, *63*, 3185–3189. (i) Markó, I. E.; Giles, P. R.; Tsukazaki, M.; Brown, S. M.; Urch, C. J. *Science* **1996**, *274*, 2044–2046.
- (3) (a) Brownell, K. R.; McCrory, C. C. L.; Chidsey, C. E. D.; Perry, R. H.; Zare, R. N.; Waymouth, R. M. *J. Am. Chem. Soc.* **2013**, *135*, 14299–14305. (b) Vannucci, A. K.; Hull, J. F.; Chen, Z.; Binstead, R. A.; Concepcion, J. J.; Meyer, T. J. *J. Am. Chem. Soc.* **2012**, *134*, 3972–3975. (c) Yamazaki, S.-i.; Yao, M.; Fujiwara, N.; Siroma, Z.; Yasuda, K.; Ioroi, T. *Chem. Commun.* **2012**, *48*, 4353–4355. (d) Serra, D.; Correia, M. C.; McElwee-White, L. *Organometallics* **2011**, *30*, 5568–5577.
- (4) (a) Hoover, J. M.; Stahl, S. S. *J. Am. Chem. Soc.* **2011**, *133*, 16901–16910. (b) Kowal, A.; Port, S. N.; Nichols, R. J. *Catal. Today* **1997**, *38*, 483–492. (c) Li, C.; Kawada, H.; Sun, X.; Xu, H.; Yoneyama, Y.; Tsubaki, N. *ChemCatChem* **2011**, *3*, 684–689.
- (5) (a) Lee, J.; Ryu, T.; Park, S.; Lee, P. H. *J. Org. Chem.* **2012**, *77*, 4821–4825. (b) Dilger, A. K.; Gopalsamuthiram, V.; Burke, S. D. *J. Am. Chem. Soc.* **2007**, *129*, 16273–16277. (c) Atwood, D. A.; Budzelaar, P. H. M.; Hutchinson, A. R.; Linton, D. J.; Schubert, D. M.; Talarico, G.; Uhl, W.; Wheatley, A. E. H.; Zhang, Y. *Group 13 Chemistry III: Industrial Applications*; Springer: Berlin, 2003; Vol. 105. (d) Liu, Y.-C.; Ko, B.-T.; Huang, B.-H.; Lin, C.-C. *Organometallics* **2002**, *21*, 2066–2069.
- (6) (a) Chng, L. L.; Chang, C. J.; Nocera, D. G. *Org. Lett.* **2003**, *5*, 2421–2424. (b) Rosenthal, J.; Nocera, D. G. *Acc. Chem. Res.* **2007**, *40*, 543–553. (c) Tronic, T. A.; Kaminsky, W.; Coggins, M. K.; Mayer, J. M. *Inorg. Chem.* **2012**, *51*, 10916–10928. (d) Bullock, R. M.; Appel, A. M.; Helm, M. L. *Chem. Commun.* **2014**, *50*, 3125–3143.
- (7) (a) Dutta, A.; Lense, S.; Hou, J.; Engelhard, M. H.; Roberts, J. A. S.; Shaw, W. J. *J. Am. Chem. Soc.* **2013**, *135*, 18490–18496. (b) Gross, M. A.; Reynal, A.; Durrant, J. R.; Reisner, E. J. *J. Am. Chem. Soc.* **2013**, *136*, 356–366. (c) Franz, J. A.; O'Hagan, M.; Ho, M.-H.; Liu, T.; Helm, M. L.; Lense, S.; DuBois, D. L.; Shaw, W. J.; Appel, A. M.; Raugei, S.; Bullock, R. M. *Organometallics* **2013**, *32*, 7034–7042. (d) Wiese, S.; Kilgore, U. J.; DuBois, D. L.; Bullock, R. M. *ACS Catal.* **2012**, *2*, 720–727. (e) O'Hagan, M.; Ho, M.-H.; Yang, J. Y.; Appel, A. M.; Rakowski DuBois, M.; Raugei, S.; Shaw, W. J.; DuBois, D. L.; Bullock, R. M. *J. Am. Chem. Soc.* **2012**, *134*, 19409–19424. (f) Kilgore, U. J.; Roberts, J. A. S.; Pool, D. H.; Appel, A. M.; Stewart, M. P.; Rakowski DuBois, M.; Dougherty, W. G.; Kassel, W. S.; Bullock, R. M.; DuBois, D. L. *J. Am. Chem. Soc.* **2011**, *133*, 5861–5872. (g) Helm, M. L.; Stewart, M. P.; Bullock, R. M.; Rakowski DuBois, M.; DuBois, D. L. *Science* **2011**, *333*, 863–866. (h) Wiedner, E. S.; Yang, J. Y.; Dougherty, W. G.; Kassel, W. S.; Bullock, R. M.; Rakowski DuBois, M.; DuBois, D. L. *Organometallics* **2010**, *29*, 5390–5401.
- (8) (a) Das, P.; Ho, M.-H.; O'Hagan, M.; Shaw, W. J.; Morris Bullock, R.; Raugei, S.; Helm, M. L. *Dalton Trans.* **2014**, *43*, 2744–2754. (b) Darmon, J. M.; Raugei, S.; Liu, T.; Hulley, E. B.; Weiss, C. J.; Bullock, R. M.; Helm, M. L. *ACS Catal.* **2014**, *4*, 1246–1260. (c) Liu, T.; DuBois, D. L.; Bullock, R. M. *Nat. Chem.* **2013**, *5*, 228–233. (d) Yang, J. Y.; Smith, S. E.; Liu, T.; Dougherty, W. G.; Hoffert, W. A.; Kassel, W. S.; Rakowski DuBois, M.; DuBois, D. L.; Bullock, R. M. *J. Am. Chem. Soc.* **2013**, *135*, 9700–9712. (e) Yang, J. Y.; Chen, S.; Dougherty, W. G.; Kassel, W. S.; Bullock, R. M.; DuBois, D. L.; Raugei, S.; Rousseau, R.; Dupuis, M.; Rakowski DuBois, M. *Chem. Commun.* **2010**, *46*, 8618–8620. (f) Wilson, A. D.; Newell, R. H.; McNevin, M. J.; Muckerman, J. T.; Rakowski DuBois, M.; DuBois, D. L. *J. Am. Chem. Soc.* **2006**, *128*, 358–366.
- (9) (a) Galan, B. R.; Reback, M. L.; Jain, A.; Appel, A. M.; Shaw, W. J. *Eur. J. Inorg. Chem.* **2013**, *2013*, 5366–5371. (b) Galan, B. R.; Schöffel, J.; Linehan, J. C.; Seu, C.; Appel, A. M.; Roberts, J. A. S.; Helm, M. L.; Kilgore, U. J.; Yang, J. Y.; DuBois, D. L.; Kubiak, C. P. *J. Am. Chem. Soc.* **2011**, *133*, 12767–12779.
- (10) Frazee, K.; Wilson, A. D.; Appel, A. M.; Rakowski DuBois, M.; DuBois, D. L. *Organometallics* **2007**, *26*, 3918–3924.
- (11) The stronger oxidant  $Cp_2FeBF_4$  oxidizes triethylamine, while  $Cp_2CoPF_6$  is not strong enough of an oxidant for catalysis.
- (12) Torriero, A. A. J.; Shiddiky, M. J. A.; Burgar, I.; Bond, A. M. *Organometallics* **2013**, *32*, 5731–5739.
- (13) The plot of kinetic data for the oxidation of diphenylmethanol catalyzed by  $Ni(P^{Pb}_2N^{Bn}_2)_2(BF_4)_2$  (**6**) contains a possible, brief induction period that may be due to one of the diphosphine ligands dissociating from the nickel center.
- (14) Complex **4** has been observed to catalytically oxidize diphenylmethanol to benzophenone without the need for base or oxidant. No  $H_2$  was detected by  $^1H$  NMR spectroscopy or GC. This behavior was not observed in complexes **1–3**. See the Supporting Information for details.
- (15) Carey, F. A.; Sundberg, R. J. *Advanced Organic Chemistry*; Kluwer Academic/ Plenum Publishers: 2000; p 823.
- (16) No Ni–CO stretches (ref 17) were observed by IR spectroscopy after the addition of methanol to compound **2**. The products appear to be paramagnetic based on NMR spectra.
- (17) Wilson, A. D.; Frazee, K.; Twamley, B.; Miller, S. M.; DuBois, D. L.; Rakowski DuBois, M. *J. Am. Chem. Soc.* **2007**, *130*, 1061–1068.
- (18) Stolley, R. M.; Darmon, J. M.; Helm, M. L. *Chem. Commun.* **2014**, *50*, 3681–3684.
- (19) Wiedner, E. S.; Yang, J. Y.; Chen, S.; Raugei, S.; Dougherty, W. G.; Kassel, W. S.; Helm, M. L.; Bullock, R. M.; Rakowski DuBois, M.; DuBois, D. L. *Organometallics* **2011**, *31*, 144–156.
- (20) (a) Kaljurand, I.; Kütt, A.; Sooväli, L.; Rodima, T.; Mäemets, V.; Leito, I.; Koppel, I. A. *J. Org. Chem.* **2005**, *70*, 1019–1028. (b) Kolthoff, I. M.; Chantooni, M. K.; Bhowmik, S. *Anal. Chem.* **1967**, *39*, 315–320.
- (21) Xue, L.; Ahlquist, M. S. G. *Inorg. Chem.* **2014**, *53*, 3281–3289.
- (22) Hathaway, B. J.; Holah, D. G.; Underhill, A. E. *J. Chem. Soc.* **1962**, 2444–2448.
- (23) Liu, T.; Wang, X.; Hoffmann, C.; DuBois, D. L.; Bullock, R. M. *Angew. Chem., Int. Ed.* **2014**, *53*, 5300–5304.
- (24) Fulmer, G. R.; Miller, A. J. M.; Sherden, N. H.; Gottlieb, H. E.; Nudelman, A.; Stoltz, B. M.; Bercaw, J. E.; Goldberg, K. I. *Organometallics* **2010**, *29*, 2176–2179.
- (25) Connelly, N. G.; Geiger, W. E. *Chem. Rev.* **1996**, *96*, 877–910.
- (26) Dolomanov, O. V.; Bourhis, L. J.; Gildea, R. J.; Howard, J. A. K.; Puschmann, H. *J. Appl. Crystallogr.* **2009**, *42*, 339–341.
- (27) Gildea, R. J.; Bourhis, L. J.; Dolomanov, O. V.; Grosse-Kunstleve, R. W.; Puschmann, H.; Adams, P. D.; Howard, J. A. K. *J. Appl. Crystallogr.* **2011**, *44*, 1259–1263.
- (28) Sheldrick, G. M. *Acta Crystallogr.* **2008**, *A64*, 112–122.